Published OnlineFirst March 9, 2010; DOI: 10.1158/1535-7163.MCT-09-0800

Research Article

Molecular Cancer Therapeutics

IFN-β Restricts Tumor Growth and Sensitizes Alveolar Rhabdomyosarcoma to Ionizing Radiation

Thomas L. Sims[1,4], Mackenzie McGee[1], Regan F. Williams[1,4], Adrianne L. Myers[1,4], Lorraine Tracey[1], J. Blair Hamner[1,4], Catherine Ng[1], Jianrong Wu[2], M. Waleed Gaber[5], Beth McCarville[3], Amit C. Nathwani[6], and Andrew M. Davidoff[1,4]

Abstract

Ionizing radiation is an important component of multimodal therapy for alveolar rhabdomyosarcoma (ARMS). We sought to evaluate the ability of IFN-β to enhance the activity of ionizing radiation.

Rh-30 and Rh-41 ARMS cells were treated with IFN-β and ionizing radiation to assess synergistic effects *in vitro* and as orthotopic xenografts in CB17 severe combined immunodeficient mice. In addition to effects on tumor cell proliferation and xenograft growth, changes in the tumor microenvironment including interstitial fluid pressure, perfusion, oxygenation, and cellular histology were assessed.

A nonlinear regression model and isobologram analysis indicated that IFN-β and ionizing radiation affected antitumor synergy *in vitro* in the Rh-30 cell line; the activity was additive in the Rh-41 cell line. *In vivo* continuous delivery of IFN-β affected normalization of the dysfunctional tumor vasculature of both Rh-30 and Rh-41 ARMS xenografts, decreasing tumor interstitial fluid pressure, increasing tumor perfusion (as assessed by contrast-enhanced ultrasonography), and increasing oxygenation. Tumors treated with both IFN-β and radiation were smaller than control tumors and those treated with radiation or IFN-β alone. Additionally, treatment with high-dose IFN-β followed by radiation significantly reduced tumor size compared with radiation treatment followed by IFN-β.

The combination of IFN-β and ionizing radiation showed synergy against ARMS by sensitizing tumor cells to the cytotoxic effects of ionizing radiation and by altering tumor vasculature, thereby improving oxygenation. Therefore, IFN-β and ionizing radiation may be an effective combination for treatment of ARMS. *Mol Cancer Ther; 9(3); 761–71. ©2010 AACR.*

Introduction

Rhabdomyosarcoma is the most common soft tissue sarcoma of childhood, accounting for more than half of all soft tissue sarcomas in this patient population (1, 2). The use of multimodal therapy has resulted in substantial improvement in cure rates for patients with rhabdomyosarcoma over the past 30 years. However, particular subsets of rhabdomyosarcoma still provide significant clinical challenges. Outcomes for patients with alveolar histology rhabdomyosarcoma (ARMS), for example, continue to lag behind those for embryonal histology, with Intergroup Rhabdomyosarcoma Study-IV results indicating that 5-year failure free survival for ARMS is only 65% despite intensive therapy (3, 4).

Ionizing radiation is an integral part of multimodal therapy for rhabdomyosarcoma, especially ARMS. Radiotherapy can be used to shrink tumors before operative resection and is used to reduce recurrence by treating residual disease. Unfortunately, as with most treatments, ionizing radiation also produces dose-related side effects to surrounding normal tissue. Radiation therapy can be associated with complications, such as bone growth abnormalities, peripheral nerve injury, impaired mobility, and secondary malignancies (5). The frequency of significant late effects of radiotherapy can be as high as 80% (5). Adjuvant agents that augment the response of tumors to radiation might allow for the use of lower doses of ionizing radiation, thereby maintaining efficacy while decreasing toxicity.

One promising adjuvant agent is IFN-β. IFN-β inhibits tumor growth through diverse mechanisms of action including direct tumor cell toxicity (6), upregulation of apoptosis (7), and inhibition of angiogenesis (8–10). Recently, we have shown that continuous delivery of IFN-β affects tumor angiogenesis by "normalizing" the dysfunctional tumor vasculature, decreasing vessel permeability and interstitial fluid pressure, and improving

Authors' Affiliations: Departments of [1]Surgery, [2]Biostatistics, and [3]Radiologic Sciences, St. Jude Children's Research Hospital; Departments of [4]Surgery and [5]Biomedical Engineering, University of Tennessee Health Science Center, Memphis, Tennessee and [6]Department of Hematology/Oncology, University College, London, United Kingdom

Corresponding Author: Andrew M. Davidoff, St. Jude Children's Research Hospital, 262 Danny Thomas Place, Memphis, TN 38105. Phone: 901-595-3741; Fax: 901-595-6621. E-mail: andrew.davidoff@stjude.org

doi: 10.1158/1535-7163.MCT-09-0800

Published OnlineFirst March 9, 2010; DOI: 10.1158/1535-7163.MCT-09-0800

intratumoral blood flow. This, in turn, improves tumor oxygenation (11).

Although the benefit of improving the perfusion and oxygenation of tumors may seem counterintuitive, tumor oxygenation has an important impact on the effectiveness of ionizing radiation (12). Ionizing radiation kills tumor cells through the generation of oxygen free radicals, which cause DNA injury leading to apoptosis. Hypoxia has been shown to interfere with the cytotoxic effects of ionizing radiation as well as contribute to the emergence of radiation-resistant tumor cells (13, 14). Achieving the same level of tumor cell killing requires three times the radiation dose under hypoxic conditions compared with normal states (12). Hyperbaric oxygen (15), erythropoietin (16), alterations in hemoglobin affinity for oxygen (17), and blood transfusions (18) are therapies that have been tried to improve intratumoral oxygenation and thereby improve tumor response to radiation. These approaches have had mixed results, however. This may be because each of these therapies changes the oxygen content within the blood, but if blood is not being delivered efficiently throughout a tumor, the effect of the interventions will be minimized.

Tumor angiogenesis results in an uneven distribution of blood vessels and perfusion throughout a tumor. Some areas of a tumor then become necrotic and hypoxic providing pockets of resistance to radiation therapy. The poor vessel quality inherently produced by tumor angiogenesis also results in leaky vessels, which increase the intratumoral interstitial pressure, compressing small vessels and further reducing perfusion throughout the tumor. Because ionizing radiation kills tumor cells through the creation of oxygen free radicals, increased perfusion and oxygenation of tumors should increase cell death in response to radiation therapy. Based on our prior experience, continuous delivery of IFN-β may produce this desired effect (11). In addition, IFN-β has been shown to enhance the efficacy of radiation on several tumor cell lines *in vitro* through a direct effect (19). Importantly, in that same study, IFN-β did not seem to increase the toxicity of radiation on nonmalignant cells (19). We, therefore, hypothesized that treating alveolar rhabdomyosarcoma xenografts with IFN-β before radiation would result in greater antitumor response to radiation.

Materials and Methods

In vitro Analysis

Rh-30 and Rh-41 cell lines were provided by Dr. P. Houghton (St. Jude Children's Research Hospital). These cell lines had retained the histologic appearance of alveolar rhabdomyosarcoma and were tested by short tandem repeat analysis when initially derived (20). Sensitivity to IFN-β was established using an MTS assay (CellTiter 96 AQueous One Solution, Promega). Cells were treated for a total of 96 h with 10 to 10,000 units of recombinant human IFN-β (Avonex, Biogen Idec, Inc.) given daily. All measurements were done with 12 replicates. To analyze the effects of IFN-β on cell cycle and apoptosis in these lines, cells were treated with 10 to 10,000 units of recombinant human IFN-β daily for 72 h, after which time cells were analyzed by flow cytometry for DNA content and Annexin V staining. All measurements were done in triplicate.

For *in vitro* radiosensitization studies, cells were treated with recombinant human IFN-β (Avonex) at concentrations of 30 to 3,000 IU/mL and incubated for 24 h before irradiation, as described by Schmidberger et al. (19). Cells were irradiated with a cesium-137 source at single doses of 0, 1, 2, or 4 Gy. Media were changed in all flasks following irradiation to discontinue the exposure to IFN-β.

A standard colony-forming assay was used to assess cell survival. All treatment groups with varying combinations (4 × 5 factorial design) of radiation and IFN-β doses were maintained in culture for 10 d following treatment. Cells were fixed with methanol and stained with Giemsa (Sigma-Aldrich). Twenty dose combinations of IFN-β and radiation were evaluated, and each experiment was done with six replicates. An individual surviving colony was scored if >50 cells were present.

Adeno-Associated Virus Vector Production

Adeno-associated virus vectors (AAV) were used to establish continuous, long-term delivery of human IFN-β *in vivo*. Construction of the pAV2 hIFN-β and pAV2 FIX (human clotting factor IX) vector plasmids has been described previously (21). AAV-FIX served as a control vector. These vector plasmids include the CMV-IE enhancer, β-actin promoter, a chicken β-actin/rabbit β-globin composite intron, and a rabbit β-globin polyadenylation signal mediating the expression of the cDNA for human IFN-β. The hIFN-β cDNA was purchased from InvivoGen. Recombinant AAV vectors pseudotyped with serotype 8 capsid were generated by the method described previously using the pAAV8-2 plasmid provided by J. Wilson (22). These AAV2/8 vectors were purified using ion exchange chromatography (23).

Murine Tumor Model

Orthotopic (IM) ARMS xenografts were established in male CB17 severe combined immunodeficient mice (Charles River Laboratory) by injection of 2×10^6 Rh-30 or Rh-41 tumor cells in 200 μL PBS into the right calf muscle during the administration of 2% isoflurane. The size of the IM tumors was estimated by measuring the size of the normal left calf and subtracting that volume from the tumor-injected right calf volume. Measurements were done weekly in two dimensions using handheld calipers, and volumes calculated as width^2 × length × 0.5. Mice were size matched at ~3 wk after tumor cell injection and divided into groups of five to eight mice per treatment group. IFN-β treatment was accomplished by tail vein injection of AAV vector particles in a volume of 200 μL of PBS. Mice were treated with either 2.34×10^9 or 4.66×10^{10} genomic copies (gc) of AAV-2/8-CAG-hIFN-β,

Published OnlineFirst March 9, 2010; DOI: 10.1158/1535-7163.MCT-09-0800

AAV-2/8-hFIX, or no treatment. Systemic levels of human IFN-β in mouse plasma were determined 10 d after administration using a commercially available immunoassay (ELISA; Biosource International). IFN-β levels in protein extracted from tumor lysates were also measured using ELISA. Ionizing radiation was given as a single dose of 2, 4, 6, 8, 10, 12, or 15 Gy via an Orthovoltage D3000 X-ray tube (Gulmay Medical Ltd.). Mice were sacrificed, and tumor tissue was harvested 21 d after the initiation of therapy. All murine experiments were done in accordance with a protocol approved by the Institutional Animal Care and Use Committee of St. Jude Children's Research Hospital.

Tumor Interstitial Fluid Pressure

Interstitial fluid pressure was measured in the tumors of sedated mice using a needle-pressure technique, which has previously been described (24). The width of each tumor was measured, and a 23-gauge hollow bore needle was inserted into the tumor to a depth equal to one-third of the width, ensuring placement well within the tumor, but not directly in the potentially necrotic tumor center. Data are reported in cm H_2O (1 cm H_2O = 1.36 mm Hg).

Contrast-Enhanced Ultrasonography

Definity ultrasound contrast agent (Bristol-Myers Squibb) was used to perform contrast-enhanced ultrasonography on a Vevo 770 (Visual Sonics, Toronto, Ontario) small animal ultrasound machine using a 40-MHz linear transducer. Definity is a suspension of perflutren lipid microspheres designed for clinical use in echocardiography. Mean microsphere size ranges from 1.1 to 3.3 μm, and particles remain in the intravascular space. Ultrasound images were obtained while the mouse was sedated with 2% isoflurane with body temperature being maintained by a heat lamp and heated ultrasound platform. The ultrasound transducer was centered over the largest tumor area and held in that position throughout image acquisition. One hundred microliters of Definity mixed 1:1 with sterile PBS was injected into the venous system by retro-orbital injection. Imaging was recorded on a cine-clip beginning immediately before the contrast injection and continued for 60 s at a frame rate of 14 to 18 Hz. A region of interest was drawn to encompass the entire tumor, and the cine clip was evaluated for change in tumor signal intensity from pre–contrast-enhanced baseline to initial peak enhancement (ΔSI in decibels, dB).

In vivo Oxygen Tension Measurement

Tumor oxygen tension levels were measured *in vivo* using the OxyLab fiber optic probe (Oxford Optronics). The OxyLab system probe is coated in ruthenium pigment, which is excited by the fiber optic blue light. Oxygen quenches the excitation providing a calculation of the oxygen pressure in mm Hg. Mice were anesthetized with ketamine mixed with xylazine and normal saline. While sedated, the mice were placed on two liters of continuous flow oxygen by nose cone. A 23-gauge needle was inserted across the diameter of the tumor at its midpoint. The needle was then withdrawn ~5 mm, and the probe was inserted through the lumen of the needle. Oxygen pressure was measured at 5-min intervals for 25 min, and a steady-state level was recorded.

Tumor Immunohistochemistry

Formalin-fixed, paraffin-embedded 4-μm-thick tumor sections were stained with rat anti-mouse CD34 (RAM 34, Pharmingen) and mouse anti-human smooth muscle actin (SMA; clone 1A4, DAKO) antibodies as previously described by Spurbeck et al. (25). Stained tumor sections were viewed and digitally photographed using an Olympus U-SPT microscope equipped with both fluorescence and brightfield illumination with an attached CCD camera. Images were saved as JPEG files for further processing in Adobe Photoshop (Adobe Systems, Inc.). Four images at 400× were taken of each tumor section with care to avoid areas of necrosis. Positive staining was quantified using NIH image analysis software (Image J) and is reported as the mean number of positive pixels/tumor section. Apoptosis in tumors was determined by terminal deoxynucleotidyl transferase-mediated dUTP nick end labeling using a commercially available *in situ* apoptosis detection kit (Serologicals). Densities of apoptotic cells were determined by 400× light microscopy in the field with the highest density of apoptotic cells in a region that had no evidence of necrosis. Three high-power fields per tumor were counted with a minimum of 3,000 cells per tumor counted. The number of apoptotic cells per 1,000 cells was recorded.

Statistical Analyses

An approach based on isobolograms was used to assess the *in vitro* synergy between IFN-β and radiation (26, 27). A weighed nonlinear dose-response model (27) using the SAS NLIN procedure was used to fit colony survival data. Observed three-dimensional dose-response plots, fitted dose-response plots, and isobolograms were generated. Dose-independent synergy of combined ionizing radiation and IFN-β was estimated from the model by the nonadditivity parameter, α, which indicates synergism ($\alpha > 0$), antagonism ($\alpha < 0$), or no interaction ($\alpha = 0$). Additionally, data from cell lines indicating synergy by the α parameter were analyzed for dose-dependent synergy using Hewlett's joint potency ratio, *R*, with corresponding assessment of 10%, 50%, and 90% pharmacologic effect (28). The pharmacologic effect was defined as $100\ [(E_{max} - E) / (E_{max} - B)]\%$, wherein E_{max} and *B* are model parameters for the maximal and minimal effects. *E* is the mean response, which is a function of doses, and makes the pharmacologic effect a function of doses as well.

All other results are reported as mean ± SEM. Increase in dB of contrast enhancement from baseline to peak perfusion was analyzed with Mann-Whitney *U* test in SAS statistical software. The Sigmaplot program (SPSS, Inc.) was used to analyze and graphically present all other data. An unpaired Student's *t* test was used to analyze statistical differences in the *in vivo* experimental results.

Published OnlineFirst March 9, 2010; DOI: 10.1158/1535-7163.MCT-09-0800

Results

Effect of Recombinant IFN-β on Alveolar Rhabdomyosarcoma Cells *In vitro*

Rh-41 and Rh-30 cells were analyzed for their sensitivity to IFN-β using an MTS viability assay (Fig. 1A). Both lines were sensitive, although there were some differences observed in cell cycle and apoptotic response to IFN-β (Fig. 1B). Rh-30, which exhibited greater sensitivity to IFN-β, showed a dramatic and highly significant increase in the percentage of cells in S phase at IFN-β concentrations at as low as 100 units/mL. However, no significant increase in apoptosis was observed in the Rh-30 cell line. Rh-41 cells, which were somewhat less sensitive to IFN-β, showed a modest yet statistically significant increase in the percentage of cells in S phase as well as a doubling of Annexin V–positive apoptotic cells when treated with concentrations of IFN-β at ≥100 units/mL.

Analysis of Synergism between IFN-β and Radiation Therapy in ARMS Cell Lines *In vitro*

Plotting the individual colony counts for each cell line after treatment provided a three-dimensional contour map of the response to treatment for that cell line with the Rh-30 cells producing more overall colonies (Fig. 2A). A weighed nonlinear dose-response model was fitted to each cell line (Fig. 2B), and the model fit was highly significant for both cell lines ($P < 0.001$). IFN-β and ionizing radiation (X-ray therapy, XRT) showed synergy against the Rh-30 cell line, producing a positive α, nonadditivity, parameter of 1.34 [95% confidence interval (CI 95% CI), 0.70–1.98]. For treatment of the Rh-41 cells, however, the α parameter was 0.229 (95% CI, −0.078 to 0.537). Because the confidence interval included 0 in the Rh-41 cell line, we cannot definitely conclude that synergy between IFN-β and radiation therapy occurred in these cells; however, the effects were additive.

Dose-dependent synergy was evaluated using Hewlett's joint potency ratios, *R*, corresponding to 10%, 50%, and 90% pharmacologic effects. *R* values in the Rh-30 model were 1.08, 1.26, and 1.71, thereby showing more synergy with higher dose combinations. The corresponding isobolograms for this model show bowing contours that give a visual indication of the degree of synergy (Fig. 2C). Synergy was not observed between IFN-β and radiation in the Rh-41 cell line; however, additivity was seen and an isobologram was included to visually represent the additivity (Fig. 2C). The Hewlett's joint potency ratios corresponding to 10%, 50%, and 90% pharmacologic effects were 1.01, 1.05, and 1.27 for the Rh-41 cell line.

Rhabdomyosarcoma Animal Model and Treatment Course

Orthotopic human Rh-30 ARMS tumors were established in the right calf muscles of CB17 severe combined

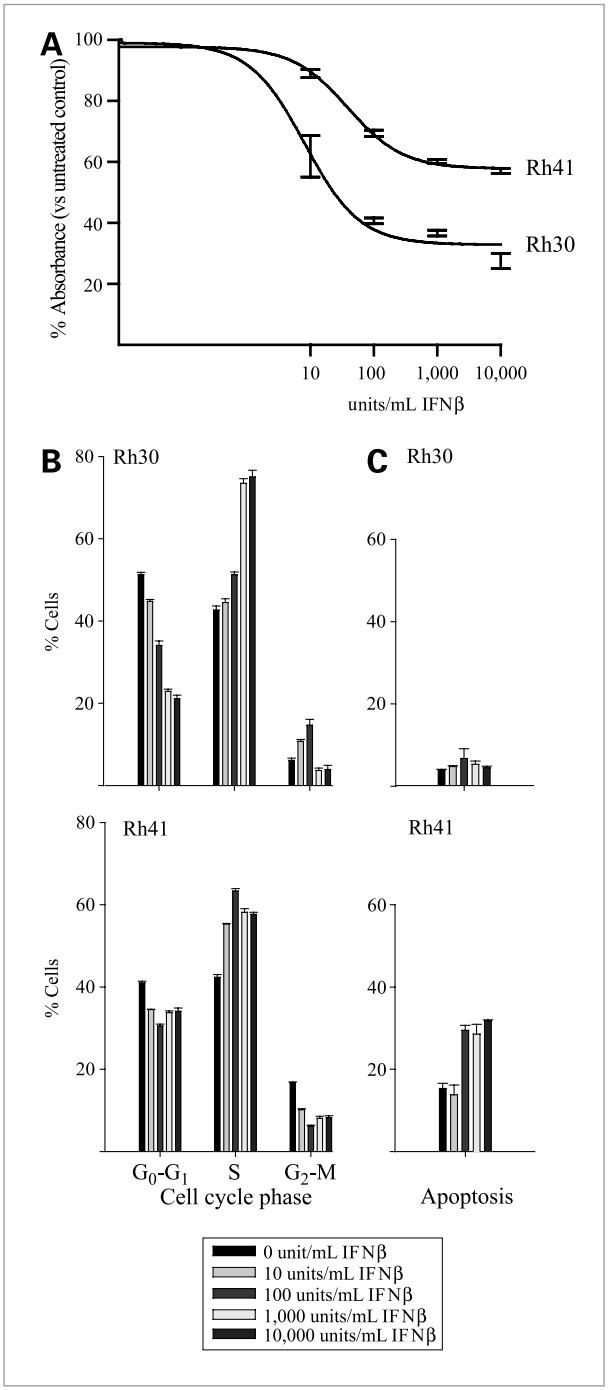

Figure 1. *In vitro* effects of IFN-β on alveolar rhabdomyosarcoma cell lines. A, sensitivity to IFN-β. Sensitivity to IFN-β was established in Rh-41 and Rh-30 cell lines using an MTS assay. Data are shown for 96 h treatments with 10 to 10,000 units of rhIFN-β. All measurements were done with 12 replicates. Points, mean; bars, SEM. B, alterations in cell cycle. Flow cytometry revealed that IFN-β causes S-phase arrest after 72 h of treatment (Rh-30, $P < 0.002$ for 100, 1,000, and 10,000 units/mL; Rh-41, $P < 0.0001$ for 10, 100, 1,000, and 10,000 units/mL). All measurements were done in triplicate. Columns, mean; bars, SEM. C, apoptosis in Rh-41 cells but not Rh-30 cells. Flow cytometry for Annexin V staining revealed that IFN-β causes apoptosis in Rh-41 cells ($P < 0.01$ for 100, 1,000, and 10,000 units/mL); no significant change was observed in the Rh-30 cell line. All measurements were done in triplicate. Columns, mean; bars, SEM.

Published OnlineFirst March 9, 2010; DOI: 10.1158/1535-7163.MCT-09-0800

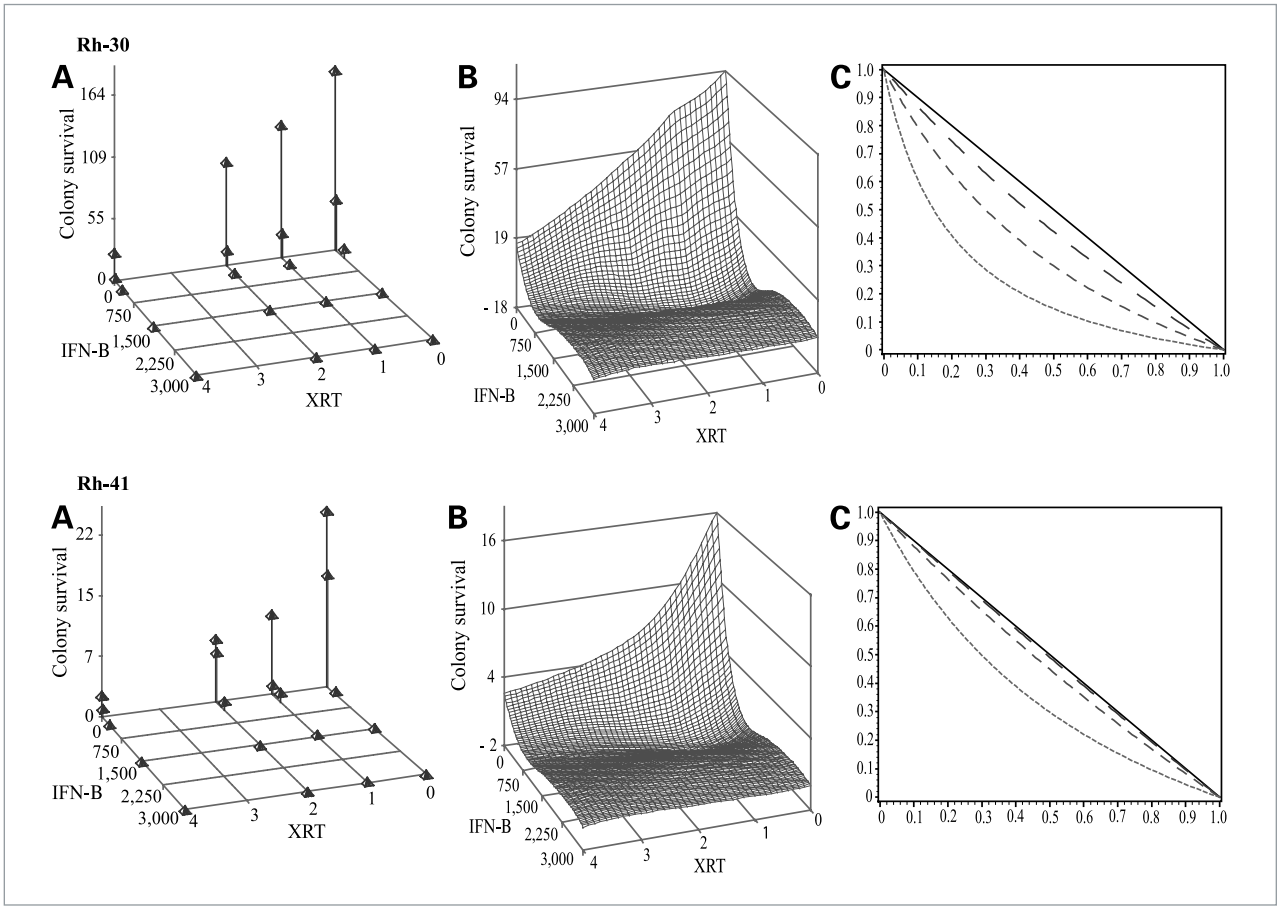

Figure 2. Evaluation of *in vitro* synergy between IFN-β and radiation in the treatment of alveolar rhabdomyosarcoma cell lines. A, observed three-dimensional colony survival surface. Actual colony survival data were averaged. B, predicted three-dimensional colony survival surface. Weighed nonlinear dose-response surface models of colony survival data for IFN-β plus ionizing radiation (XRT) in both cell lines were estimated from fitting the joint potency model equation. The model fit was good for both cell lines ($P < 0.001$). Dose-independent synergy of combined therapy was estimated from the model by the nonadditivity parameter, α, which indicates synergism ($\alpha > 0$), antagonism ($\alpha < 0$), or no interaction ($\alpha = 0$). IFN-β and XRT showed synergy against the Rh-30 cell line, producing a positive α, nonadditivity parameter of 1.34 (95% CI, 0.70–1.98). The α parameter for Rh-41 cells was 0.229 (95% CI, −0.78 to 0.527), showing only additivity, not synergy, because the confidence interval included zero. C, isobolograms corresponding to 10% (large dashes), 50% (medium dashes), and 90% (small dashes) pharmacologic effect. Both cell lines were analyzed for dose-dependent synergy using Hewlett's joint potency ratio, *R*, with corresponding assessment of 10%, 50%, and 90% pharmacologic effect. *R* values for the Rh-30 model were 1.08, 1.26, and 1.71, indicating increased synergy with increasing dose combinations. *R* values for the Rh-41 model were 1.01, 1.05, and 1.27, indicating only additivity.

immunodeficient mice. These tumors mimicked ARMS behavior in humans with an infiltrative growth pattern (Fig. 3A). After ~3 weeks of growth, mice were size-matched by tumor volume into groups of eight mice each. One group served as an untreated control, one group was treated at 3 weeks of tumor growth with AAV-IFN-β (2.34×10^9 gc/mouse) only, one group received radiation treatment (4 Gy) only, and one group received AAV-IFN-β (2.34×10^9 gc) followed 1 week later by radiation treatment. Mice were sacrificed, and tissue was harvested 21 days after the initiation of treatment, which was the end point of the study. To evaluate the extent to which treatment efficacy was due to IFN-β–mediated vascular changes and sensitization of tumor cells before radiation or simply a combination of two treatment effects, an additional group was treated with radiation followed by AAV-IFN-β (2.34×10^9 gc) 1 week later. Human IFN-β was undetectable in the plasma of all untreated control mice and all mice were treated only with radiation, but mice treated with AAV-IFN-β had an average systemic level of human IFN-β of 335 ± 82 pg/mL 10 days after administration.

Maturation of the Tumor Vessels in IFN-β–Treated ARMS Xenografts

Twenty-one days after the initiation of treatment, five Rh-30 tumor-bearing mice per treatment group were euthanized and tumor tissue was harvested for staining. Immunohistochemical analysis was done to evaluate the effect of continuous IFN-β therapy on the tumor vasculature at the cellular level. As we have previously observed in neuroblastoma xenografts (11), there was a

Published OnlineFirst March 9, 2010; DOI: 10.1158/1535-7163.MCT-09-0800

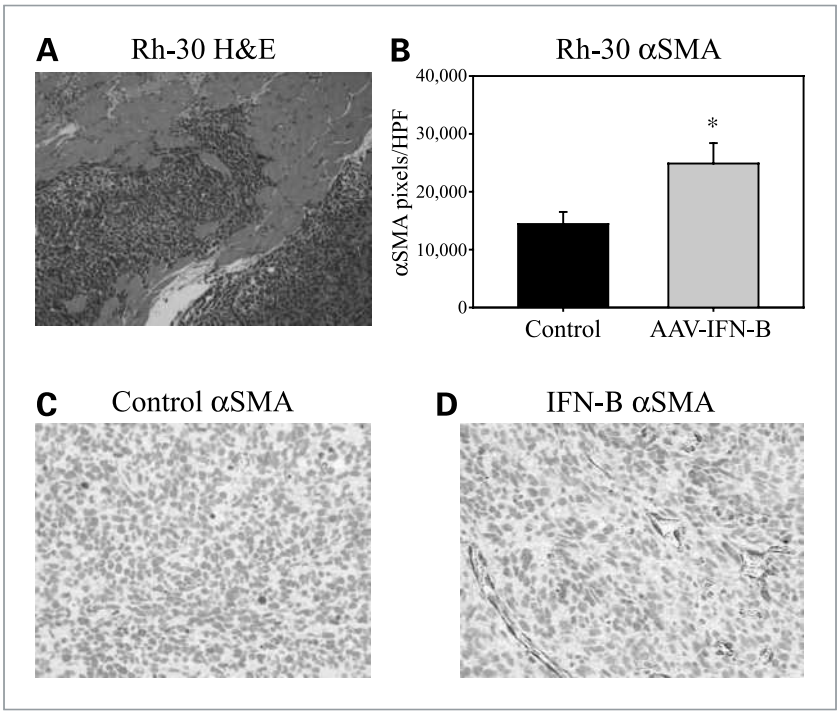

Figure 3. Tumor histology and immunohistochemistry. A, Rh-30 micrograph. Representative image of an orthotopic, IM Rh-30 alveolar rhabdomyosarcoma xenograft stained with H&E (10×). B, α-SMA staining after treatment with IFN-β. IFN-β–treated tumors had a significantly higher number of perivascular stabilizing cells than control tumors (24,873 ± 3,541 versus 14,419 ± 2,095 pixels/HPF; *, $P = 0.02$). C, representative micrograph of α-SMA (dark) immunohistochemical staining for perivascular stabilizing cells in tumors (lighter background cells) from control mice (40×). D, representative micrograph of α-SMA immunohistochemical staining for perivascular stabilizing cells in tumors from IFN-β–treated mice (40×).

significant increase in the number of intratumoral vascular smooth muscle cells (VSMC), as identified by their positive α-SMA staining, with IFN-β treatment [24,873 ± 3,531 pixels/high power field (HPF)]. In contrast, the vessels in control tumors had much less VSMC investment (14,419 ± 2,095 pixels/HPF, $P = 0.02$; Fig. 3B; representative α-SMA slides are shown in Fig. 3C and D). Also previously observed in neuroblastoma xenografts (11), there was a significant increase in the number of endothelial cells, as identified by CD34 staining, in the IFN-β–treated group (104,694 ± 33,145 pixels/HPF) compared with control tumors (15,976 ± 1,648 pixels/HPF, $P = 0.02$; Fig. 4). This increase in both endothelial cells and VSMCs suggests stabilization of tumor vasculature after treatment with IFN-β (representative CD34 slides of Rh-30 control and IFN-β–treated slides are shown in Fig. 4B and C).

Decreased Interstitial Fluid Pressure in IFN-β–Treated ARMS Xenografts

The paucity of VSMCs in tumors is often associated with unstable, leaky vessels, which can result in increased edema within tumors. With increasing edema, there is increasing interstitial fluid pressure, which is thought to cause the collapse of smaller blood vessels, thereby hindering tumor perfusion. Interstitial fluid pressure (Fig. 5A) measured 1 week after treatment in the Rh-30 tumors of mice treated with AAV-IFN-β (2.34×10^9 gc) was 3.1 ± 0.47 cm H_2O, which was significantly lower

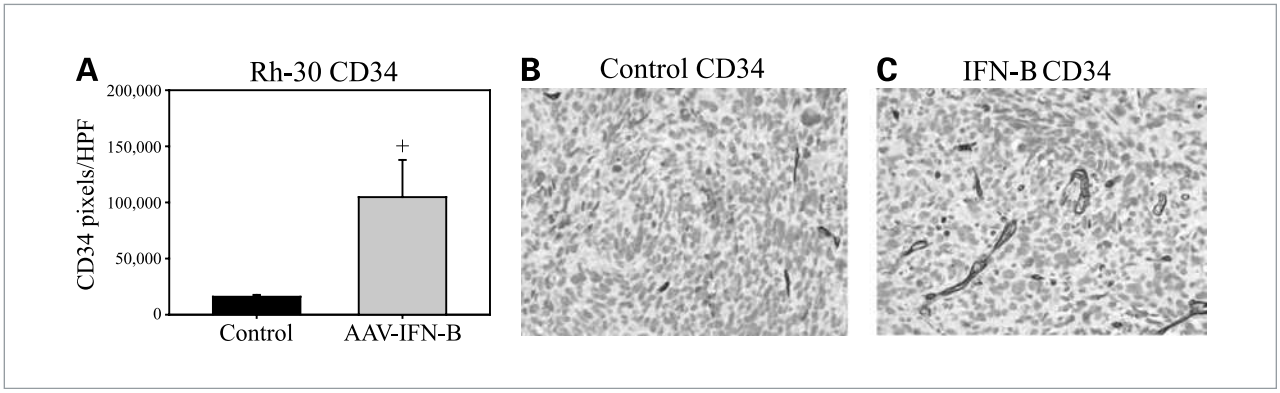

Figure 4. CD34 tumor immunohistochemistry. A, increased number of endothelial cells in IFN-β–treated tumors. IFN-β–treated tumors had significantly more endothelial cells (104,694 ± 33,145 pixels/HPF) than control tumors (15,976 ± 1,648 pixels/HPF; +, $P = 0.02$). B, representative micrograph of CD34 (dark) immunohistochemical staining for endothelial cells in a control mouse (40×). C, representative micrograph of CD34 staining for endothelial cells in an IFN-β–treated mouse (40×).

Published OnlineFirst March 9, 2010; DOI: 10.1158/1535-7163.MCT-09-0800

than the interstitial pressure in the tumors of untreated mice (9.6 ± 2.7 cm H_2O, $P = 0.007$). A dose-response relationship was observed as higher doses of AAV-IFN-β (4.66×10^{10} gc) resulted in an even further decrease in interstitial pressure (0.1 ± 0.95 cm H_2O, $P = 0.011$).

Improved Perfusion and Oxygenation in IFN-β–Treated ARMS Xenografts

We have previously shown that contrast-enhanced ultrasound can be used to evaluate changes in tumor perfusion (12). Six days after the administration of ionizing radiation or AAV-IFN-β and one day before treatment with the second agent in the combination therapy groups, tumor perfusion was evaluated with contrast-enhanced ultrasound. The change in signal intensity from baseline to peak was 1.4 times greater in tumors treated with IFN-β (53.3 ± 4.9 dB) compared with untreated tumors (36.8 ± 4.6 dB, $P = 0.023$) in the Rh-30 tumors. The change in signal intensity for the Rh-41 tumors was 2.6 times higher in tumors treated with IFN-β (135.1 ± 28.5 dB) versus untreated tumors (52.8 ± 11.5 dB, $P = 0.02$; Fig. 5B). These data suggest that tumors treated with IFN-β had significantly greater perfusion than control tumors in both tumor lines (representative contrast-enhanced images from IFN-β–treated and control mice are presented in Fig. 5C).

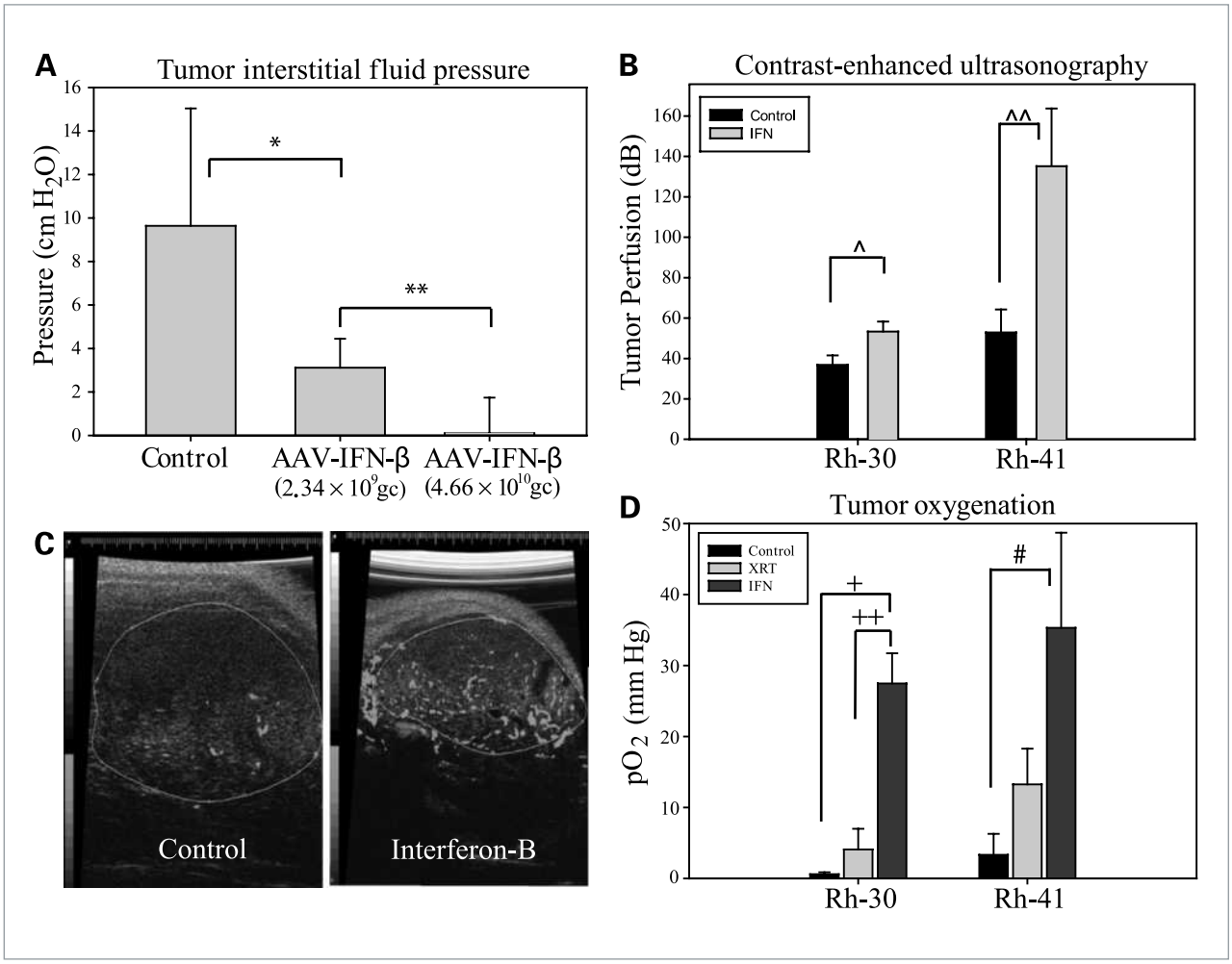

Figure 5. Physiologic changes in alveolar rhabdomyosarcoma xenografts after treatment with IFN-β or radiation. A, interstitial fluid pressure in Rh-30 tumors. Interstitial fluid pressure 1 wk after treatment with AAV-IFN-β (2.34×10^9 gc) was 3.1 ± 0.47 cm H_2O, which was significantly lower than the interstitial pressure in the tumors of untreated mice (9.6 ± 2.7 cm H_2O; *, $P = 0.007$). Higher doses of AAV-IFN-β (4.66×10^{10} gc) resulted in even further decrease in interstitial fluid pressure (0.1 ± 0.95 cm H_2O; **, $P = 0.011$). B, perfusion shown by contrast-enhanced ultrasonography. The change in signal intensity from baseline to peak was 1.4 times greater in tumors treated with IFN-β (53.3 ± 4.9 dB) compared with untreated tumors (36.8 ± 4.6 dB; ^, $P = 0.02$) in the Rh-30 tumors. The change in signal intensity for the Rh-41 tumors was 2.6 times higher in tumors treated with IFN-β (135.1 ± 28.5 dB) versus untreated tumors (52.8 ± 11.5 dB; ^^, $P = 0.02$). C, representative control and IFN-β–treated contrast-enhanced ultrasound images. D, intratumoral oxygenation in Rh-30 and Rh-41 tumors. The partial pressure of oxygen in Rh-30 tumors treated with IFN-β (27.5 ± 4.3 mm Hg) was significantly higher than untreated tumors (0.6 ± 0.3 mm Hg; +, $P < 0.001$) or radiation-treated tumors (4.1 ± 2.9 mm Hg; ++, $P = 0.001$). Rh-41 tumors also had a significantly higher intratumoral oxygenation than controls (35.3 ± 13.4 mm Hg versus 3.3 ± 2.9 mm Hg; #, $P < 0.05$).

Published OnlineFirst March 9, 2010; DOI: 10.1158/1535-7163.MCT-09-0800

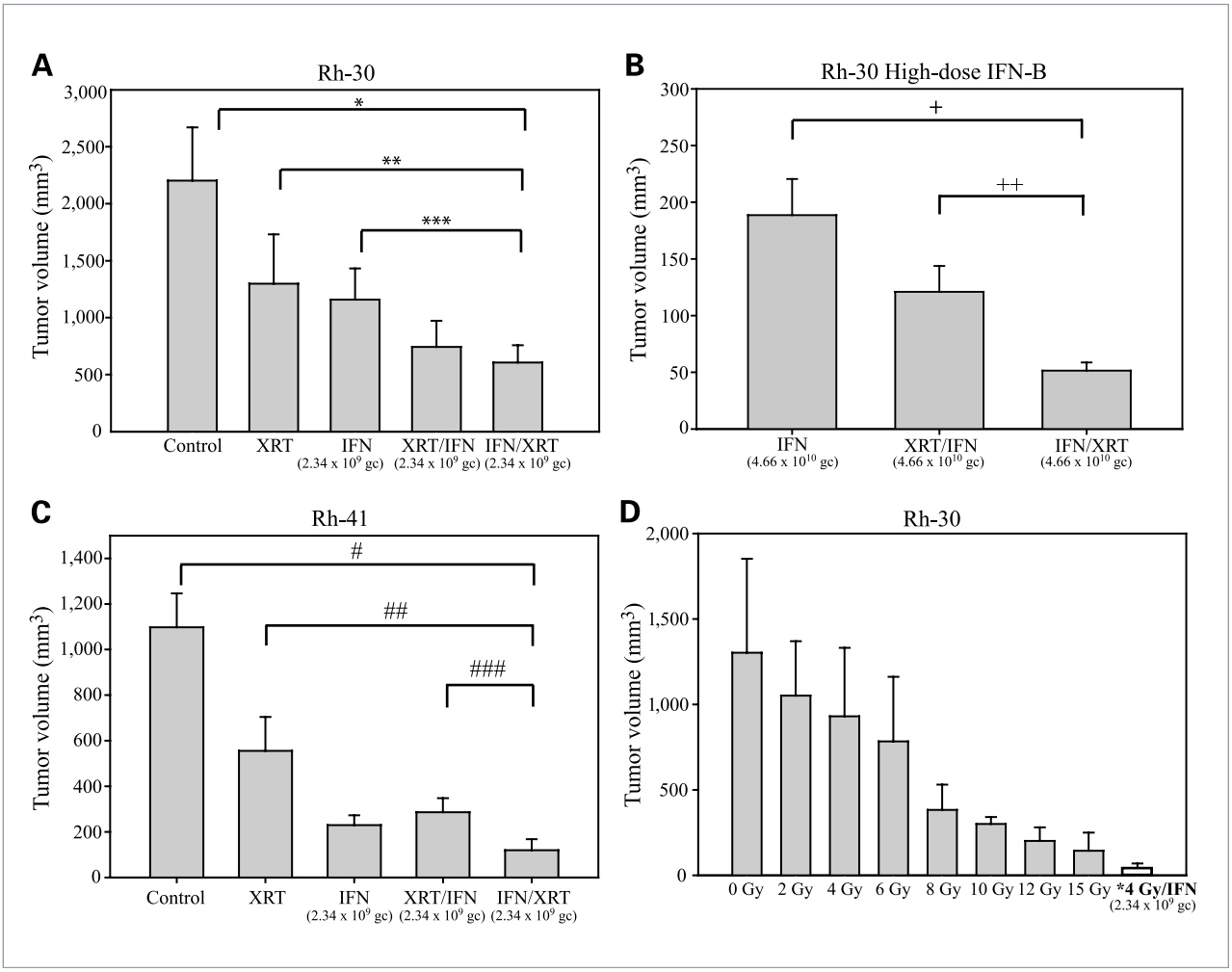

Figure 6. Treatment results of alveolar rhabdomyosarcoma xenografts. A, Rh-30 mean tumor volumes 21 d after the initiation of treatment. Tumor volumes after combination therapy with AAV-IFN-β before radiation (605.9 ± 67.7 mm^3) were significantly less than the tumor volumes in the control group (2,203.1 ± 176.4 mm^3; *, $P < 0.001$) and in mice that received either radiation alone (1,298.4 ± 153.4 mm^3; **, $P = 0.006$) or IFN-β alone (1,157.4 ± 123 mm^3; ***, $P = 0.004$). B, Rh-30 mean tumor volumes after high-dose IFN alone and in combination with XRT. Tumors treated with high-dose IFN-β before radiation were significantly smaller (51.5 ± 7.2 mm^3) than tumors treated with radiation before high-dose IFN-β (121.0 ± 22.8 mm^3; ++, $P = 0.002$) and tumors treated with high-dose IFN-β alone (188.7 ± 31.8; +, $P = 0.0001$). C, Rh-41 mean tumor volumes. Tumors treated with IFN-β before radiation showed decreased tumor volume (119.1 ± 43.8 mm^3) when compared with untreated tumors (1,097.4 ± 149.2; #, $P = 0.0002$), tumors treated with radiation only (555.6 ± 148.5 mm^3; ##, $P = 0.01$) and radiation before IFN-β (286.1 ± 61.4 mm^3; ###, $P = 0.05$). Although tumor volumes in mice treated with combination therapy were smaller than those mice treated with IFN-β alone (228.9 ± 43.8 mm^3, $P = 0.12$), the difference did not reach statistical significance. D, results of Rh-30 tumors treated with increasingly larger doses of radiation. Even at the highest single doses of radiation, tested tumors were larger than when IFN-β was given before 4-Gy irradiation, showing that pretreatment with IFN-β lowered the dose of radiation necessary to achieve the same therapeutic effect of radiation alone by 75%. Columns, mean volume of tumors treated with 4 Gy radiation after pretreatment with AAV-IFN-β.

Given the improved tumor perfusion seen with IFN-β, we hypothesized that IFN-β–treated tumors would also have increased oxygenation; therefore, the following day tumors were tested with the OxyLab probe to determine intratumoral oxygen tension (Fig. 5D). Using the Oxylab probe inserted directly in orthotopic tumors, we found that the partial pressure of oxygen in Rh-30 tumors treated with IFN-β (27.5 ± 4.3 mm Hg) was significantly higher than untreated tumors (0.6 ± 0.3 mm Hg, $P < 0.001$) or radiation-treated tumors (4.1 ± 2.9 mm Hg, $P = 0.001$). Rh-41 tumors also had a significantly higher intratumoral oxygenation than controls (35.3 ± 13.4 versus 3.3 ± 2.9 mm Hg, $P < 0.05$; Fig. 5D).

AAV-IFN-β–Mediated Vascular Maturation Improves Tumor Response to Radiation

Whereas it may seem counterintuitive to view increased tumor oxygenation as a desired effect of a treatment, the important role of oxygen in effective radiation cell killing led us to propose that increased oxygenation would correlate with increased response to radiation. IM Rh-30 xenografts treated with continuous IFN-β alone showed

Published OnlineFirst March 9, 2010; DOI: 10.1158/1535-7163.MCT-09-0800

slowed progression of tumor volume (Fig. 6A), as did tumors treated with radiation alone. The greatest growth restriction, however, occurred in mice treated with combination therapy. Tumor volume with the combination therapy of AAV-IFN-β before radiation (605.9 ± 67.7 mm^3) was significantly less than the tumor volume in the control group (2,203.1 ± 176.4 mm^3, $P < 0.001$) and in mice that received either radiation alone (1,298.4 ± 153.4 mm^3, $P = 0.006$) or IFN-β alone (1,157.4 ± 123 mm^3, $P = 0.004$).

To further explore the hypothesis that pretreatment with IFN-β may be important in enhancing tumor response to radiation, the experiment was repeated with high dose of AAV IFN-B (4.66×10^{10} gc) alone or given either 1 week before or 1 week after XRT. We hypothesized that a higher dose of AAV-IFN-β would have a greater effect on tumor vasculature, which was supported by previous data showing a greater decrease in tumor interstitial fluid pressure in tumors treated with high-dose AAV-IFN-β (4.66×10^{10} gc) compared with low-dose AAV-IFN-β (2.34×10^9 gc; Fig. 5A). Systemic levels of IFN-β were a mean of 17.6 ± 1.0 ng/mL with this dose. Intratumoral IFN-β levels in tumors treated with high-dose IFN-β were on average 50.5 ± 3.8 pg/mg total protein compared with control tumors with 0.0 pg/mg total protein. Both combination therapy groups showed tumor regression; however, tumors treated with radiation following pretreatment with high-dose IFN-β were significantly smaller (51.5 ± 7.2 mm^3) than tumors treated with radiation before IFN-β (121.0 ± 22.8 mm^3, $P = 0.002$) and tumors treated with high-dose IFN-β alone (188 ± 31.8 mm^3, $P = 0.00001$; Fig. 6B). Tumors treated with radiation before IFN-β were not significantly smaller than tumors treated with IFN-β alone ($P = 0.1$). The improved response with IFN-β given before XRT compared with IFN-β given after XRT suggests that the timing of AAV-IFN-β in relation to radiation treatment is important.

Rh-41 xenografts treated with IFN-β before radiation also showed decreased tumor volumes (119.1 ± 43.8 mm^3) when compared with untreated tumors (1,097.4 ± 149.2 mm^3, $P = 0.0002$), tumors treated with radiation only (555.6 ± 148.5 mm^3, $P = 0.01$), and radiation before IFN-β (286.1 ± 61.4 mm^3, $P = 0.05$; Fig. 6C). Tumor volumes in mice treated with combination therapy were smaller than those mice treated with IFN-β alone (228.9 ± 43.8 mm^3, $P = 0.12$), although the difference did not reach statistical significance.

To ensure that the AAV vector itself had no effect on tumor vascular phenotype or xenograft growth, mice with Rh-30 i.m. tumors were divided into two groups of five mice and received either no treatment or AAV-FIX (4.66×10^{10} gc). The same methods described above were used to determine vascular smooth muscle investment, endothelial cell density, tumor perfusion, intratumoral oxygenation, and tumor volumes. Tumors treated with the control vector did not have a statistically different number of VSMCs (51,939 ± 12,199 versus 58,559 ± 8,151 pixels/HPF) or endothelial cells (49,249 ± 5,652 versus 43,930 ± 1,136 pixels/HPF) when compared with untreated controls. AAV-FIX–treated tumors did not have a significantly different change in signal intensity compared with untreated controls (76.7 ± 10.4 versus 66.8 ± 11.9 dB) or a significantly different intratumoral oxygenation compared with untreated controls (1.3 ± 0.4 versus 1.4 ± 0.2 mm Hg). AAV-FIX–treated tumors were also not significantly different in size from untreated controls (825.8 ± 248.1 versus 622.8 ± 269.4 mm^3).

Finally, to determine whether pretreatment with IFN-β could lower the necessary dose of radiation required for tumor shrinkage, thereby, potentially limiting the toxicity of radiation therapy, increasing levels of radiation were given to additional cohorts (four mice per cohort) of size-matched Rh-30 tumors. At the highest single doses of radiation tested, tumors were still larger than when IFN-β was given before 4-Gy radiation (Fig. 6D), showing that pretreatment with IFN-β lowered the dose of radiation necessary to achieve the same therapeutic effect of radiation alone by 75%; the mice treated with this combination showed no detectable signs of toxicity.

Discussion

Several investigators have found that type I IFNs sensitize various tumor cell lines to the cytotoxic effects of ionizing radiation (19, 29–31). Our study shows that this also occurs in alveolar rhabdomyosarcoma cells. Our results also suggest an additional mechanism for the increased response to radiation following treatment with IFN-β *in vivo*. IFN-β–mediated changes in tumor vasculature seem to improve the perfusion and oxygenation of ARMS tumors, and this increased oxygenation was associated with an improved response to ionizing radiation.

Although new blood vessel formation occurs to support tumor growth, these vessels are generally very abnormal, with disorganized structure and function (32–34). On a cellular level, there are often fewer stabilizing perivascular cells resulting in highly permeable vessels and increased intratumoral interstitial fluid pressure. These abnormal blood vessels provide inefficient perfusion of the tumor. Consequently, areas of tumor that are hypoxic, acidotic, and often necrotic develop. Drug delivery is poor and radiation is ineffective in the resultant tumor microenvironment, because these modalities require adequate tissue oxygenation, target cell proliferation, and, in the case of chemotherapy, local delivery to achieve maximal antitumor efficacy.

As early as the 1970s investigators showed that angiogenesis inhibitors could enhance the antitumor effect of other chemotherapeutic agents when given in conjunction with these agents, likely through improved perfusion of the tumor (35, 36). "Normalization" of the tumor vasculature is a possible explanation for this paradoxical synergy between antiangiogenic drugs and cytotoxic agents (35–37). We have previously shown that continuous delivery of IFN-β can effect normalization of the vasculature in neuroblastoma leading to improved

Published OnlineFirst March 9, 2010; DOI: 10.1158/1535-7163.MCT-09-0800

antitumor effect when combined with traditional chemotherapeutic agents (11). Treatment with IFN-β was associated with an increase in the number of stabilizing smooth muscle cells per endothelial cell, which fortified the tumor blood vessels and increased delivery of topotecan to the tumor. A similar increase in stabilizing smooth muscle cells was also seen when Rh-30 alveolar rhabdomyosarcoma xenografts were treated with IFN-β. IFN-β also decreased the interstitial fluid pressure within the tumor, likely through the process of vascular normalization. More stable, thicker-walled, less tortuous vessels would be expected to leak less fluid into the interstitial space. Decreased interstitial fluid pressure may allow better perfusion of the tumor especially through low pressure capillaries.

Whether secondary to decreased interstitial fluid pressure or another effect of vascular normalization, treatment with IFN-β was associated with increased perfusion of ARMS tumors, as indicated by increased contrast enhancement on ultrasound and better tumor oxygenation in both Rh-30 and Rh-41 tumors. This increased oxygenation is important for improving the effectiveness of radiation therapy, because ionizing radiation kills tumor cells through the generation of oxygen free radicals. Indeed, treatment with IFN-β was associated with increased tumor oxygen tension and increased tumor response to radiation in our study, even more so when IFN-β was given before ionizing radiation. This trend was also observed in the Rh-41 cell line with combined therapy having an additive effect, although it was not synergistic *in vitro*. This implies that *in vivo* there were changes effected by IFN-β that were independent of its direct effect on tumor cells, involving a more complex mechanism.

In conclusion, IFN-β was shown to have direct toxicity to alveolar rhabdomyosarcoma and sensitized cells of this histologic type to ionizing radiation *in vitro*. *In vivo* continuous IFN-β also seemed to effect maturation of tumor vasculature, which resulted in a decrease in interstitial fluid pressure while increasing the perfusion and oxygenation of rhabdomyosarcoma xenografts. This likely contributed to the improved tumor response to ionizing irradiation, although the timing of the administration of these two agents is important. Based on these results, IFN-β and radiation therapy may be effective in the clinical treatment of alveolar rhabdomyosarcoma.

Disclosure of Potential Conflicts of Interest

No potential conflicts of interest were disclosed.

Acknowledgments

We thank St. Jude Children's Research Hospital Animal Imaging Center for ultrasound assistance, St. Jude Children's Research Hospital Vector Core Lab for the adeno-associated virus vectors, Dr. Surender Rajasekaran for the use of interstitial fluid pressure monitoring equipment, and Dodie Bush for assistance with immunohistochemistry.

The costs of publication of this article were defrayed in part by the payment of page charges. This article must therefore be hereby marked *advertisement* in accordance with 18 U.S.C. Section 1734 solely to indicate this fact.

Received 08/28/2009; revised 01/21/2010; accepted 01/21/2010; published OnlineFirst 03/02/2010.

References

1. Pastore G, Peris-Bonet R, Carli M, et al. Childhood soft tissue sarcomas incidence and survival in European children (1978–1997): report from the Automated Childhood Cancer Information System project. Eur J Cancer 2006;42:2136–49.
2. Ries LG, Smith MA, Gurney JG, et al. Cancer incidence and survival among children and adolescents: United States SEER program 1975-1995, National Cancer Institute, SEER Program. NIH Pub No 99-4649 1999.
3. Meza JL, Anderson J, Pappo AS, Meyer WH. Analysis of prognostic factors in patients with nonmetastatic rhabdomyosarcoma treated on intergroup rhabdomyosarcoma studies III and IV: the Children's Oncology Group. J Clin Oncol 2006;24:3844–51.
4. Crist WM, Anderson JR, Meza JL, et al. Intergroup rhabdomyosarcoma study: IV. Results for patients with nonmetastatic disease. J Clin Oncol 2001;19:3091–102.
5. Paulino AC. Late effects of radiotherapy for pediatric extremity sarcomas. Int J Radiat Oncol Biol Phys 2004;60:265–74.
6. Stark GR, Kerr IM, Williams BR, Silverman RH, Schreiber RD. How cells respond to interferons. Annu Rev Biochem 1998;67:227–64.
7. Lokshin A, Mayotte JE, Levitt ML. Mechanism of interferon β-induced squamous differentiation and programmed cell death in human non-small-cell lung cancer cell lines. J Natl Cancer Inst 1995;87:206–12.
8. Dvorak HF, Gresser I. Microvascular injury in pathogenesis of interferon-induced necrosis of subcutaneous tumors in mice. J Natl Cancer Inst 1989;81:497–502.
9. Izawa JI, Sweeney P, Perrotte P, et al. Inhibition of tumorigenicity and metastasis of human bladder cancer growing in athymic mice by interferon-β gene therapy results partially from various antiangiogenic effects including endothelial cell apoptosis. Clin Cancer Res 2002;8:1258–70.
10. Streck CJ, Dickson PV, Ng CY, et al. Adeno-associated virus vector-mediated systemic delivery of IFN-β combined with low-dose cyclophosphamide affects tumor regression in murine neuroblastoma models. Clin Cancer Res 2005;11:6020–9.
11. Dickson PV, Hamner JB, Streck CJ, et al. Continuous delivery of IFN-β promotes sustained maturation of intratumoral vasculature. Mol Cancer Res 2007;5:531–42.
12. Overgaard J. Hypoxic radiosensitization: adored and ignored. J Clin Oncol 2007;25:4066–74.
13. Gray LH, Conger AD, Ebert M, Hornsey S, Scott OC. The concentration of oxygen dissolved in tissues at the time of irradiation as a factor in radiotherapy. Br J Radiol 1953;26:638–48.
14. Shipley WU, Stanley JA, Steel GG. Enhanced tumor cell radiosensitivity in artificial pulmonary metastases of the Lewis lung carcinoma. Int J Radiat Oncol Biol Phys 1976;1:261–6.
15. Bennett M, Feldmeier J, Smee R, Milross C. Hyperbaric oxygenation for tumour sensitisation to radiotherapy. Cochrane Database Syst Rev 2005:CD005007.
16. Bokemeyer C, Aapro MS, Courdi A, et al. EORTC guidelines for the use of erythropoietic proteins in anaemic patients with cancer: 2006 update. Eur J Cancer 2007;43:258–70.
17. Hirst DG, Wood PJ, Schwartz HC. The modification of hemoglobin affinity for oxygen and tumor radiosensitivity by antilipidemic drugs. Radiat Res 1987;112:164–72.
18. Poskitt TR. Radiation therapy and the role of red blood cell transfusion. Cancer Invest 1987;5:231–6.
19. Schmidberger H, Rave-Frank M, Lehmann J, et al. The combined

Published OnlineFirst March 9, 2010; DOI: 10.1158/1535-7163.MCT-09-0800

effect of interferon β and radiation on five human tumor cell lines and embryonal lung fibroblasts. Int J Radiat Oncol Biol Phys 1999;43:405–12.
20. Neale G, Su X, Morton CL, et al. Molecular characterization of the pediatric preclinical testing panel. Clin Cancer Res 2008;14:4572–83.
21. Streck CJ, Zhang Y, Miyamoto R, et al. Restriction of neuroblastoma angiogenesis and growth by interferon-α/β. Surgery 2004;136:183–9.
22. Davidoff AM, Ng CY, Zhou J, Spence Y, Nathwani AC. Sex significantly influences transduction of murine liver by recombinant adeno-associated viral vectors through an androgen-dependent pathway. Blood 2003;102:480–8.
23. Davidoff AM, Ng CY, Sleep S, et al. Purification of recombinant adeno-associated virus type 8 vectors by ion exchange chromatography generates clinical grade vector stock. J Virol Methods 2004;121:209–15.
24. Dickson PV, Hamner JB, Sims TL, et al. Bevacizumab-induced transient remodeling of the vasculature in neuroblastoma xenografts results in improved delivery and efficacy of systemically administered chemotherapy. Clin Cancer Res 2007;13:3942–50.
25. Spurbeck WW, Ng CY, Strom TS, Vanin EF, Davidoff AM. Enforced expression of tissue inhibitor of matrix metalloproteinase-3 affects functional capillary morphogenesis and inhibits tumor growth in a murine tumor model. Blood 2002;100:3361–8.
26. Greco WR, Park HS, Rustum YM. Application of a new approach for the quantitation of drug synergism to the combination of *cis*-diamminedichloroplatinum and 1-β-D-arabinofuranosylcytosine. Cancer Res 1990;50:5318–27.
27. Machado SG, Robinson GA. A direct, general approach based on isobolograms for assessing the joint action of drugs in pre-clinical experiments. Stat Med 1994;13:2289–309.
28. Hewlett PS. Measurement of the potencies of drug mixtures. Biometrics 1969;25:477–87.
29. Gerweck LE, Zaidi ST, Delaney TF. Enhancement of fractionated-dose irradiation by retinoic acid plus interferon. Int J Radiat Oncol Biol Phys 1998;42:611–5.
30. Gruninger L, Cottin E, Li YX, et al. Sensitizing human cervical cancer cells *In vitro* to ionizing radiation with interferon β or γ. Radiat Res 1999;152:493–8.
31. Gould MN, Kakria RC, Olson S, Borden EC. Radiosensitization of human bronchogenic carcinoma cells by interferon β. J Interferon Res 1984;4:123–8.
32. Carmeliet P, Jain RK. Angiogenesis in cancer and other diseases. Nature 2000;407:249–57.
33. Folkman J. Role of angiogenesis in tumor growth and metastasis. Semin Oncol 2002;29:15–8.
34. Fidler IJ, Ellis LM. Neoplastic angiogenesis-not all blood vessels are created equal. N Engl J Med 2004;351:215–6.
35. Le Serve AW, Hellmann K. Metastases and the normalization of tumour blood vessels by ICRF 159: a new type of drug action. Br Med J 1972;1:597–601.
36. Teicher BA, Holden SA, Ara G, et al. Potentiation of cytotoxic cancer therapies by TNP-470 alone and with other anti-angiogenic agents. Int J Cancer 1994;57:920–5.
37. Jain RK. Normalizing tumor vasculature with anti-angiogenic therapy: a new paradigm for combination therapy. Nat Med 2001;7:987–9.

Published OnlineFirst March 9, 2010; DOI: 10.1158/1535-7163.MCT-09-0800

Molecular Cancer Therapeutics

IFN-β Restricts Tumor Growth and Sensitizes Alveolar Rhabdomyosarcoma to Ionizing Radiation

Thomas L. Sims, Mackenzie McGee, Regan F. Williams, et al.

Mol Cancer Ther 2010;9:761-771. Published OnlineFirst March 9, 2010.